

# Critical states observed in triaxial compression tests on volcanic pumice soil related to debris flow in the 2008 Iwate-Miyagi Nairiku Earthquake

Hiroyuki Hashimoto<sup>1\*</sup>, Itsuki Sato<sup>2</sup>, and Reiko Kuwano<sup>3</sup>

<sup>1</sup>The University of Tokyo, Department of civil engineering, 7-3-1 Hongo, Bunkyo, Tokyo, Japan

<sup>2</sup>Port and Airport Research Institute, Geotechnical Engineering Department, 3-1-1 Nagase, Yokosuka, Kanagawa, Japan

<sup>3</sup>The University of Tokyo, Institute of Industrial Science, 4-6-1 Komaba, Meguro, Tokyo, Japan

**Abstract.** The Iwate-Miyagi Nairiku Earthquake (M7.2) that occurred on June 14, 2008, caused a slope failure in Dozo-zawa River near the summit of Mt. Higashi-Kurikoma. The debris flow caused by the slope failure flowed for about 10 km and took the lives of 7 people. The mechanisms of the slope failure and long-distance debris flow have not yet been well understood. In this study, a series of triaxial compression tests was conducted using a highly crushable pumice soil collected from the collapsed area, and shear behavior and particle breakage were discussed. Both reconstituted specimens and intact specimens showed contractancy and reached critical states that implies high flow potential. However, intact specimens preserved looser structure during consolidation and showed stronger contractancy during shearing than the reconstituted specimens, due to their natural soil structure. Significant particle breakage was observed in the tests with reconstituted specimens.

## 1 Introduction

### 1.1 Dozou-sawa slope failure and debris flow

The Iwate-Miyagi Nairiku Earthquake of magnitude 7.2 hit an inland volcanic mountain area in Northern Japan on June 14, 2008. As a result of the earthquake, a large slope failure was generated at the head of Dozou-sawa river near the top of Mt. Higashi Kurikoma, as shown in Figs. 1(a) and (b). The scale of the slope failure was estimated to be about 200 m long, 300 m in maximum width, and 30 m in maximum thickness with about 1.5 million m<sup>3</sup> in volume of debris [1]. This slope failure triggered a debris flow that travelled 10 km and 7 people were killed in Koma-no-yu hot spring.

The collapse site is part of the Quaternary Kurikoma volcano. The geology around the area is composed of andesitic lava, tuff, and fused tuff, and the bedrock is Neogene sedimentary rock, tuff, and fused tuff [2]. As shown in Fig. 1(c), non-welded brown pumice soil and weathered volcanic clay were found on the slip cliff and ground surface in the northern part of the collapse area.

### 1.2 Properties of Dozou-sawa pumice soil

A particle of the Dozou-sawa brown pumice soil was porous and contained water within it. It could be easily crushed by fingers, and when crushed, the water in the particle came out and became sticky.

The particle size distribution and physical properties of the pumice soil are shown in Fig. 2 and Table 1, respectively. The particle sizes of the soil were generally in the range of 0.1 to 10 mm. The dry density of Dozou-sawa pumice soil measured at the site was below 1, and void ratio was 1.84, indicating that the soil had an extremely loose structure. Plasticity index was examined using particles sieved to less than 425 micrometers and found to be as low as 7. The reason the natural water content ( $w_n$ ) became higher than the liquid limit ( $w_l$ ) is considered that the original pumice soil contained coarser particles than those used in the liquid limit test, and the coarser particles trapped more water in their intra-particle voids.

### 1.3 Research objective

In this study, a series of triaxial tests was conducted on intact and reconstituted specimens of Dozou-sawa pumice soil to investigate mechanisms of the large slope failure and long-distance debris flow. Particle breakage was also discussed by examining the particle size distributions of the specimens before and after the tests.

**Table 1.** Physical properties of Dozou-sawa pumice soil

$\rho_s$ (g/cm <sup>3</sup> )	$\rho_d$ (g/cm <sup>3</sup> )	$w_n$ (%)	$e$	$D_{50}$ (mm)	$w_p$ (%)	$w_L$ (%)	$I_p$ (%)
2.66	0.93	62	1.84	1.7	53	60	7

$\rho_s$ : Soil particle density,  $\rho_d$ : Dry density,  $w_n$ : Water content in natural condition,  $e$ : Void ratio,  $D_{50}$ : Mean particle diameter,  $w_p$ : Plastic limit,  $w_L$ : Liquid limit,  $I_p$ : Plasticity index

\* Corresponding author: [hsmt@iis.u-tokyo.ac.jp](mailto:hsmt@iis.u-tokyo.ac.jp)

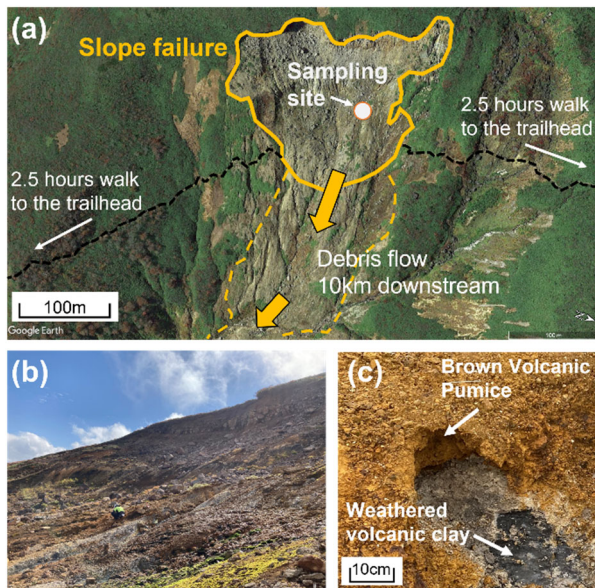


**Fig. 1.** Slope failure in Dozou-sawa river: (a) Google Earth image, (b) General view, (c) Exposed volcanic pumice soil

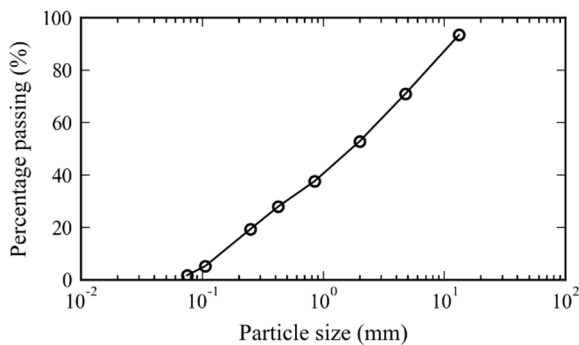


**Fig. 2.** In-situ particle size distribution of Dozou-sawa pumice soil

## 2 Triaxial tests

### 2.1 Specimen preparation

To examine the effect of soil structure, intact specimens (less disturbed specimens that maintained the in-situ soil structure) and reconstituted specimens were prepared in this study.

Intact samples were collected at the site by pushing tubes gently in a vertical direction into the target layer. They were extracted from the tubes, trimmed to cylindrical specimens of 50 mm in diameter and 100 mm in height, as shown in Fig. 3.

Reconstituted specimens of 50 mm in diameter and 100 mm in height were made of disturbed sample that had been naturally dried and passed through a 13.2 mm sieve, as shown in Fig. 3. The soils were re-mixed to match the particle size distribution of the natural condition. To minimize the particle breakage during the sample preparation, each specimen was prepared in 5 layers by spooning the soil into the mold and applying gentle tamping until a target void ratio was achieved. The specimens were prepared to be roughly equal to the in-situ void ratio (target  $e=1.8$ ) using naturally dried soil,

except for one case, where the target void ratio was 2.2 using slightly moist soil.

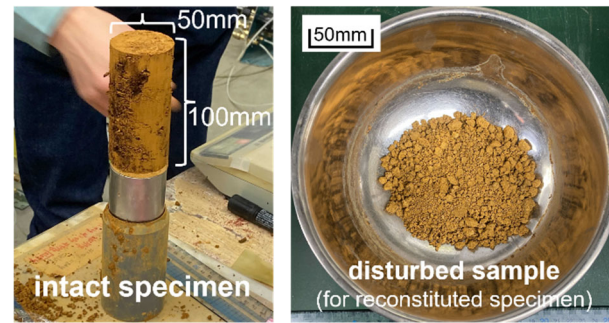


**Fig. 3.** Intact specimen and disturbed sample for reconstituted specimen

### 2.2 Test conditions

Table 2 summarizes the conditions of triaxial tests in this study. A series of drained (CD) and undrained (CU) monotonic compression tests was conducted under saturated conditions. The confining pressure before consolidation was 20 kPa for intact specimens and 10 kPa for reconstituted specimens. To ensure a high degree of saturation (Skempton's B-value > 0.95), the double-vacuum method and a back pressure of 200 kPa were applied. Specimens were isotropically consolidated to 20, 100 or 200 kPa and left 1 hour to complete primary consolidation. Undrained or drained monotonic loading was then applied at a shear rate of 1.0 mm/min. After testing, specimens were oven-dried and then sieved to measure the amount of particle breakage during the tests.

In addition, one experiment (R20) was conducted in which only a reconstituted specimen was prepared and saturated to check for particle breakage due to specimen preparation, saturation, and oven drying.

**Table 2.** Test conditions of triaxial tests

Case ID	Specimen type	Test type	$\sigma'_c$ (kPa)	$e_i$	$e_c$
IU20	Intact	CU	20	1.96	1.96
IU100		CU	100	1.65	1.59
IU200		CU	200	1.85	1.67
IU200_2		CU	200	2.10	1.88
ID100		CD	100	2.07	1.95
RU20	Reconstituted	CU	20	1.76	1.75
RU100		CU	100	1.74	1.60
RU200		CU	200	1.58	1.46
RD100		CD	100	1.74	1.58
R20		Saturation	...	1.82	
RU100L	Recon loose	CU	100	2.29	1.53

$\sigma'_c$ : Effective confining pressure,  $e_i$ : Initial void ratio,  $e_c$ : Void ratio after consolidation. Note that IU100 contained a large particle approximately 30 mm in diameter.

### 2.3 Results

Fig. 4 summarizes the results of triaxial tests.

Referring to Figs. 4(a) and (b), in all the CU tests, deviator stresses,  $q$ , gradually increased with axial strains,  $\epsilon_a$ , and finally stabilized. The CU tests with reconstituted specimens initially exhibited contractancy, then passing the phase transformation point where the dilatancy behavior, the way of excessive pore water pressure generation, changed from contractive to dilative. When  $\epsilon_a$  reached 10 to 15 %, they finally reached critical states, where deformation continues under constant stress and constant volume, that implies high flow potential. The critical state line is illustrated by the dotted line in Fig. 4(b). The CU tests with intact specimens show similar behavior to reconstituted ones. Especially, in the cases of an effective confining pressure,  $e'_c$ , of 200kPa (IU200 and IU200\_2), strong contractancy was observed. The effective stress paths reached critical state without experiencing the phase transformation.

Referring to Figs. 4(a) to (c), both the CD test with intact specimen (ID100) and reconstituted specimen (RD100) exhibited a large contractancy. In the CD test with reconstituted specimen (RD100),  $q$  and volumetric strain,  $\epsilon_{vol}$ , became constant at  $\epsilon_a = 15$  %, and reached critical state. In contrast, in the CD test with intact specimen (ID100), the increase of  $q$  was more gradual, and the strong contraction continued even when  $\epsilon_a$  reached nearly 20%.

In Fig. 4(d), the void ratios,  $e$ , are plotted against the mean effective stresses,  $p'$ , in semi-logarithmic scale. A linear critical state line was observed for reconstituted specimens. The reconstituted specimen with loose initial structure (RU100L) collapsed during consolidation and came on the same critical state line. On the other hand, the intact specimens kept higher void ratios than the reconstituted specimens at the corresponding  $p'$ , indicating that the structure of intact specimens was not completely lost due to consolidation pressure.

These differences in the behavior of intact and reconstituted specimens can be attributed to dissimilarity in soil structure of the two specimen types. The loose in-situ soil structure was found to be difficult to reproduce in reconstituted specimens.

Fig. 5 shows the particle size distributions before and after triaxial tests. Significant particle breakage was observed in all the cases with reconstituted specimens. However, no relationship was found between effective confining pressure and the magnitude of particle breakage. Significant particle breakage was observed even in the test with only the specimen preparation and saturation (R20), suggesting that large particle breakage occurred before shearing. It is not clear at what stage and to what extent the crushing occurred. The intense particle breakage prior to shearing made it difficult to evaluate the effect of shear behavior on the soil structure. Particle size distributions of the intact specimens were largely varied. Since the particle size distributions before the tests were not known, the amount of particle breakage in the intact specimens could not be examined.

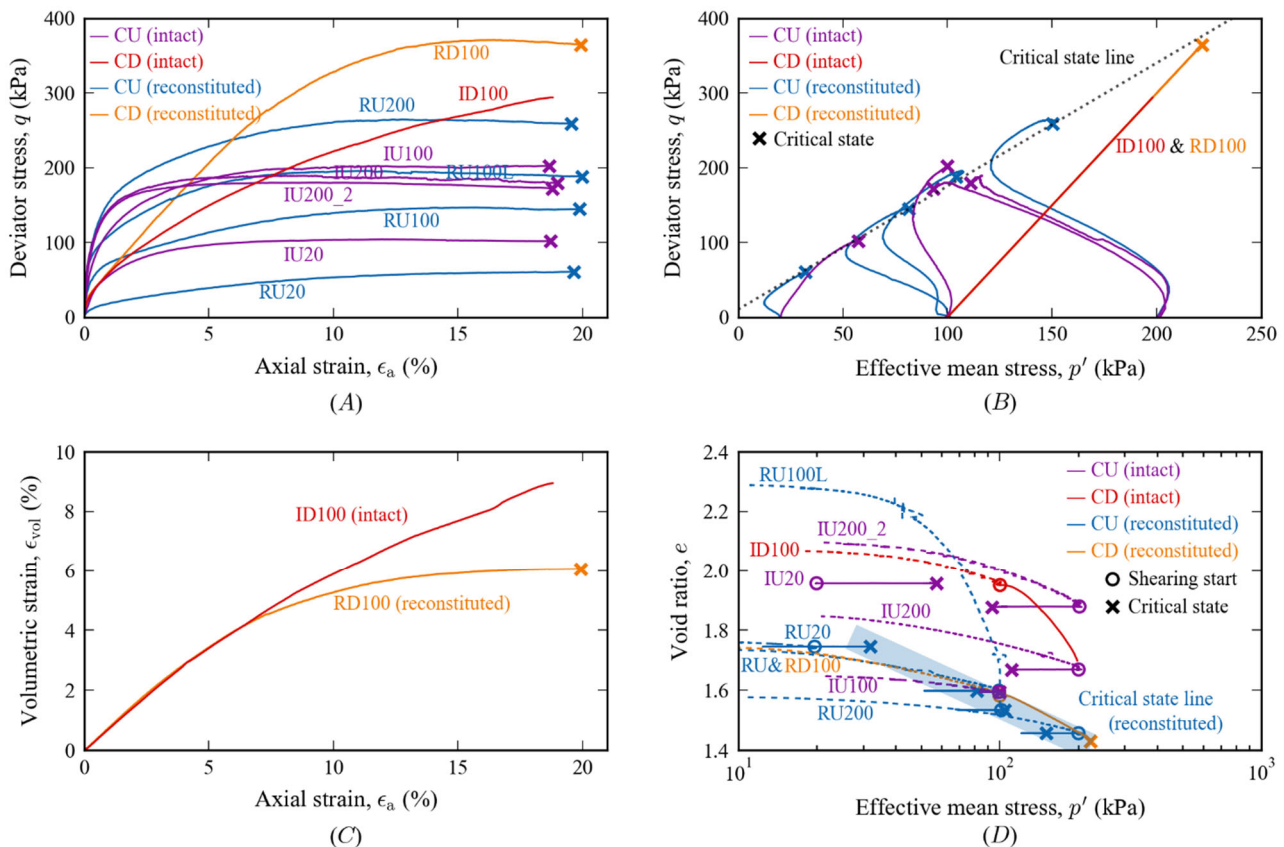


**Fig. 4.** Results of triaxial tests. (a) Deviator stress and axial strain relationship. (b) Deviator stress and effective  $p'$  mean stress relationship. (c) Volumetric strain and axial strain relationships. (d) Void ratio and Effective mean stress relationship.

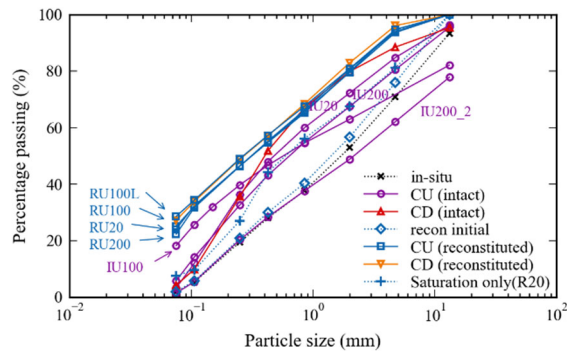


Fig. 5. Particle size distribution before and after triaxial tests

### 3 Conclusions

In this study, a series of triaxial tests were performed on the volcanic pumice soil collected in Dozou-sawa river, where a large slope failure and a long-distance debris flow occurred in the 2008 Iwate-Miyagi Nairiku Earthquake. The pumice soil was highly crushable and retained extremely loose structure in the in-situ condition. Such a loose structure could not be reproduced in a reconstituted specimen. Almost all the cases reached critical states that indicated high flow potential. Intact specimens retained looser structure during consolidation compared to reconstituted specimens, and those with larger confining pressures showed stronger contractancy during shearing. Significant particle breakage occurred in reconstituted specimens, but no notable relationship was observed between confining pressure and the amount of particle breakage. Further studies need to be carried out to evaluate when and how much particle breakage occurred during the tests.

### References

1. Geospatial Information Authority of Japan (GSI), Aero-photographs of slope failure area that caused damage to Komanoyu Hot Springs (2008)  
 Available at:  
<https://www.gsi.go.jp/johosystem/johosystem60030.html>, accessed: 05/11/2022. (in Japanese)
2. M. Irasawa, M. Ushiyama, H. Kawabe, M. Fujita, Y. Satofuka, D. Higaki, T. Uchida, A. Ikeda, J. of JSECE, **61**, 3, pp. 37-46 (2008)  
[https://doi.org/10.11475/sabo.61.3\\_37](https://doi.org/10.11475/sabo.61.3_37) (in Japanese)